

A simple rule for finding Dirac Cones in Bilayered Perovskites

XueJiao Chen,^{1,2} Lei Liu,^{1,*} and DeZhen Shen^{1,†}

¹*State Key Laboratory of Luminescence and Applications, Changchun Institute of Optics, Fine Mechanics and Physics, Chinese Academy of Sciences, No.3888 Dongnanhu Road, Changchun 130033, Peoples Republic of China*

²*University of Chinese Academy of Sciences, Beijing 100049, Peoples Republic of China*
(Dated: September 17, 2024)

We propose a simple rule for finding Dirac cone electronic states in solids, that is neglecting those lattice atoms inert to the particular electronic bands, and pursuing the two dimensional (2D) graphene-like quasi-atom lattices with *s*- and *p*-bindings by considering the equivalent atom groups in the unit cell as quasi-atoms. With CsPbBr₃ and Cs₃Bi₂Br₉ bilayers as examples, we demonstrate the effectiveness and generality of this rule with the density functional theory (DFT) calculations. We demonstrate that both bilayers have Dirac cones around the Fermi level and reveal that their corresponding Fermi velocities can reach as high as $\sim 0.2 \times 10^6$ m/s. That makes these new 2D layered materials very promising in making new ultra-fast ionic electronic devices.

“Dirac Cone”, describing the gapless linear-dispersion of electronic bands, characterizes the superior ballistic massless charge-carrier transport of solids such as in graphene¹⁻³, or on the surfaces of topological insulators⁴⁻⁶. Theoretically, the Dirac cones had been predicted in 1947 in graphene, whose honeycomb lattice of *s-p* bonding results in the conical band structure with the linearly dispersive valence and conduction bands touching each other at the Dirac points (K or K') of its hexagonal Brillouin zone¹. Nevertheless, it was only after its first isolation⁷, graphene has become a source of new sciences, and aroused research upsurges again and again over its novel electronic behaviors⁸⁻¹⁸. In fact, by energy-band theory and symmetry analysis¹, the normal Dirac cones as presented in graphene will generally appear in those materials, as long as they have the similarly honeycomb bonding style as graphene does. But, among hundreds of 2D materials examined by now, only graphynes¹⁹, silicene and germanene²⁰, ionic boron²¹, and others²² have been identified to be the normal Dirac materials. Nevertheless, unlike graphene, these 2D Dirac materials are made of some sort of artificial lattices where the atoms do not bond together as they do in their stable natural structural polymorphs. In this letter, we propose that following a simple but effective rule more Dirac cone states can be found generally in the 2D materials with stable natural bonding structures.

Here, perovskites are selected to demonstrate physics behind the rule we proposed for finding 2D Dirac materials. As shown in Fig. 1a, normally perovskites have the well-known ABX₃ lattice structure, where the 6-fold coordinated B cation and its surrounded X anions form the BX₆ octahedron, the BX₆ octahedra share their X corners forming the 3D skeleton, and the A cations occupy every hole among the 8 BX₆ octahedra. For a cubic ABX₃ lattice, if viewed from the [111] direction, it presents natively the hexagonal symmetry as shown in Fig. 1b. While the A cations stay isolated from the BX₆ skeleton, their electronic states normally do not participate in forming the low-energy bands dispersing near the Fermi level. For a selected halide perovskite

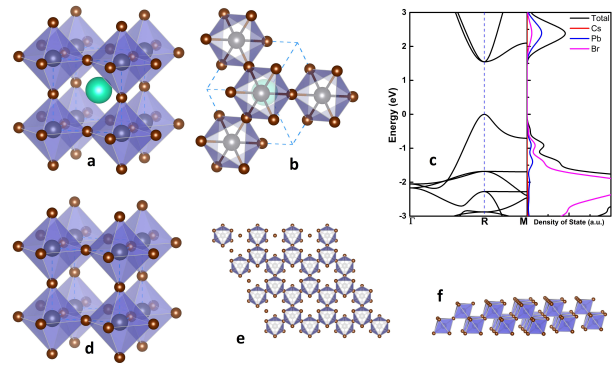


FIG. 1. **a** The crystal structure of a cubic ABX₃ perovskite, where the green, gray, and brown balls represent the A cations, B cations, and the X anions, respectively; **b** the crystal structure of a cubic perovskite, viewed from its [111] direction; **c** the calculated electronic band structure of bulk CsPbBr₃, together with its total and site-decomposed DOS; **d** the effective crystal structure of a cubic ABX₃ perovskite, effectively seen by its low energy charge carriers; **e** the top view of the crystal structure of a BX₆ bilayer sliced out along the (111) plane of a cubic perovskite, which constructs the hexagonal honeycomb lattice with two equivalent BX₆ sublattices; and **f** the side view of the crystal structure of a hexagonal BX₆ bilayer, which indeed presents a buckled single quasi-atom (BX₆) layer.

(CsPbBr₃), Fig. 1c plots its gapped electronic band structure calculated with DFT, together with the total and site-decomposed density of states (DOS). That demonstrates clearly that the electronic orbitals of the A cations stay a few electronvolts away from the valence band maximum (VBM) and the conduction band minimum (CBM) and thus play no role in deciding the low-energy electronic behaviors of a perovskite. Therefore, for those low energy charge carriers, no matter electrons or holes, propagating in a perovskite crystal, the effective lattice they see would be without A cations as shown in Fig. 1d. For such a cubic lattice, if sliced out along the (111) plane, two BX₆ layers construct naturally the

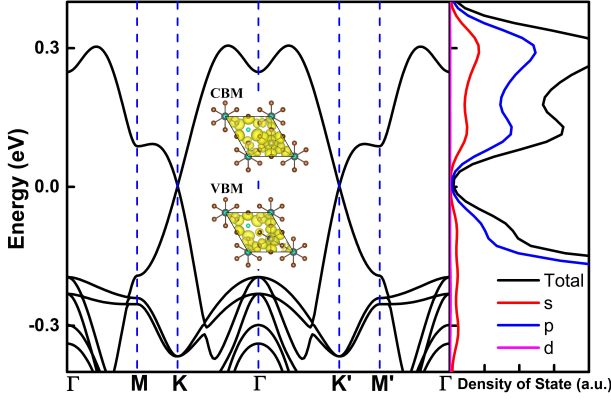


FIG. 2. The calculated electronic band structure of a hexagonal CsPbBr₃ bilayer (the insets plot the isosurfaces of VBM and CBM partial charge densities), together with its orbital-decomposed DOS.

hexagonal honeycomb lattice with two equivalent BX₆ sublattices similar as graphene as shown in Fig. 1e. If considering the BX₆ octahedron as a quasi-atom, such a BX₆ bilayer transforms into a buckled single quasi-atom layer with structure exactly like silicene²⁰ as shown in Fig. 1f.

Consequently, a hexagonal perovskite bilayer will present naturally the Dirac-cone electronic states as graphene at its Dirac points of K and K'. This is a corollary based on the honeycomb symmetry of BX₆ sublattices and the *s*- and *p*-binding characters of BX₆ octahedra¹. As a verification example, the hexagonal CsPbBr₃ bilayer was selected to calculate its electronic band structures near the Fermi level. Here, the DFT calculations were performed within Perdew-Burke-Ernzerhof (PBE) generalized gradient approximation²³ and the projected augmented wave (PAW) method²⁴, as implemented by the Vienna ab initio simulation package (VASP)^{25–27}. The cutoff energy for the plane-wave basis set is 300 eV and the Brillouin zone is sampled with the Monkhorst-Pack mesh of 6 × 6 × 6 for bulk and 6 × 6 × 1 for bilayer CsPbBr₃. The lattice parameter of bulk CsPbBr₃ is set to its experimental value $a_0 = 5.874 \text{ \AA}$ ²⁸. For the CsPbBr₃ (111) bilayer, it has the lattice constant of 8.307 Å ($\sqrt{2} \times 5.874 \text{ \AA}$) and the thickness of about 6.783 Å.

As expected, as shown in Fig. 2, its top valence and bottom conduction bands disperse linearly and touch each other at K and K' points. Their orbital-decomposed DOS reveals clearly the *s*- and *p*-orbital nature of both bands around the Dirac points. And that is evidenced further by the insets of Fig. 2 which plot the isosurfaces of VBM and CBM partial charge densities. By fitting these two bands at $\mathbf{k} = \mathbf{K} + \mathbf{q}$ to the expression $v_F \simeq E(\mathbf{q})/\hbar|\mathbf{q}|$ ²⁰, the Fermi velocity is estimated to be $v_F \sim 0.2 \times 10^6 \text{ m/s}$, which is one fifth of graphene v_F . While graphene has the intrinsic carrier mobility of 200000 cm²V⁻¹s⁻¹²⁹, it is reasonable to infer that car-

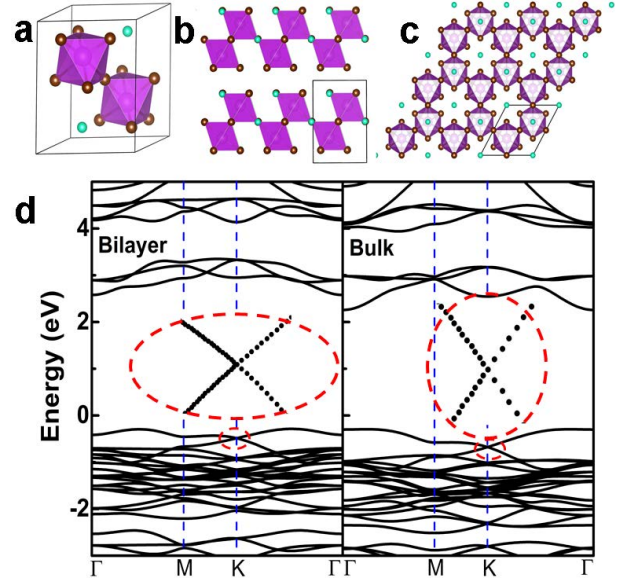


FIG. 3. The crystal structures of Cs₃Bi₂Br₉ in its primitive cell **a**, from the side view **b**, and from the top view along its natural hexagonal axis **c**; the calculated electronic band structures of bilayer **d** and bulk Cs₃Bi₂Br₉ **e**, where the insets zoom-in their Dirac bands below the Fermi level.

rier mobility in such a CsPbBr₃ bilayer may go around 40000 cm²V⁻¹s⁻¹. That makes it rather superior in making ultra-fast electronic devices in comparison with those conventional semiconductors³⁰ normally with mobilities less than 10000 cm²V⁻¹s⁻¹.

Moreover, the vacancy-order halide perovskites A₃B₂X₉ (A: Cs; B: Fe, Sb, Bi; X: Cl, Br, I) are selected to demonstrate the effectiveness of this rule to find the Dirac electronic states away from the Fermi level. Naturally, the A₃B₂X₉ perovskites are stacked together by those bilayers of linked BX₆ octahedra. Figs. 3a and 3b presents the crystal structure of Cs₃Bi₂Br₉, as an example of the vacancy-order halide perovskites. If viewed from their natural hexagonal axis, the A₃B₂X₉ perovskites present the honeycomb lattice of BX₆ quasi-atoms, as shown in Fig. 3c. Experimentally, the bulk Cs₃Bi₂Br₉ crystals had been successfully grown by dissolving Bi(OH)₃ and Cs₂CO₃ in a dilute HBr solution, in 1977 by Lazarini et al³¹. This layered material presents the trigonal symmetry with space group of P $\bar{3}$ m1 and lattice constants of $a = 7.972 \text{ \AA}$ and $c = 9.867 \text{ \AA}$ ³¹. As a stacking unit, its bilayer is inherently stable as graphene to graphite or single-layer h-BN to bulk h-BN. Based on the similar quasi-atom analysis on the CsPbBr₃ bilayer, the Cs₃Bi₂Br₉ bilayer will certainly present the Dirac electronic states as well.

Fig. 3d shows the calculated electronic band structure of the Cs₃Bi₂Br₉ bilayer. And as expected, it presents the crossing Dirac bands as well. However, as Bi contributes one more electron in Cs₃Bi₂Br₉ than Pb does in CsPbBr₃, its Fermi level goes above the Dirac bands

for the $\text{Cs}_3\text{Bi}_2\text{Br}_9$ bilayer. Its Fermi velocity at the crossing point is found to be $v_F \sim 0.2 \times 10^6 \text{ m/s}$, which equals to the values of the CsPbBr_3 bilayer. Furthermore, as the layer interaction is rather weak in bulk $\text{Cs}_3\text{Bi}_2\text{Br}_9$, its electronic band structure presents the similar Dirac bands below the Fermi level, as shown in Fig. 3e. It is notable that the electronic band structures of $\text{A}_3\text{B}_2\text{X}_9$ perovskites have been calculated previously, such as on $\text{Cs}_3\text{Bi}_2\text{Br}_9$ ³², or on $\text{Cs}_3\text{Sb}_2\text{I}_9$ ³³. But, in these works, the Dirac-band features of their band structures had been neither noticed or pointed out.

In conclusion, we propose a quasi-atom rule for searching 2D Dirac materials in the conventional solids with natural stable bonding lattices. With this rule, we demonstrate with DFT calculations that hexagonal perovskite ABX_3 bilayers, such as the CsPbBr_3 (111) bi-

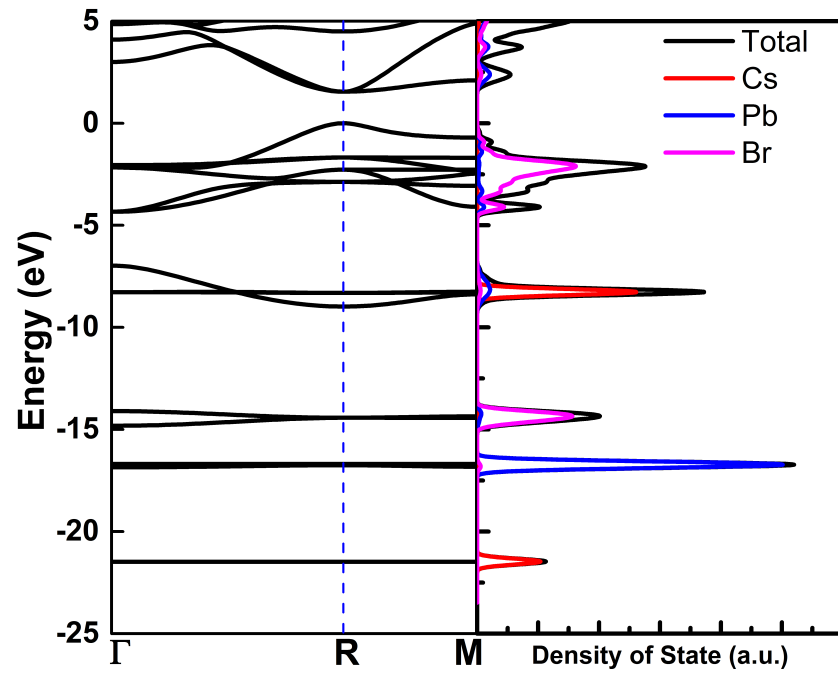
layer, may have the Dirac band crossing at the Fermi level. Similarly, taking $\text{Cs}_3\text{Bi}_2\text{Br}_9$ as an example, we demonstrate further the hexagonal vacancy-order halide perovskite $\text{A}_3\text{B}_2\text{X}_9$ bilayers, together with their bulk phases, will have the Dirac bands below the Fermi level. Both bilayer CsPbBr_3 and $\text{Cs}_3\text{Bi}_2\text{Br}_9$ layers exhibit the Fermi velocity of $\sim 0.2 \times 10^6 \text{ m/s}$. That makes them promising in making ultra-fast electronic devices.

ACKNOWLEDGMENTS

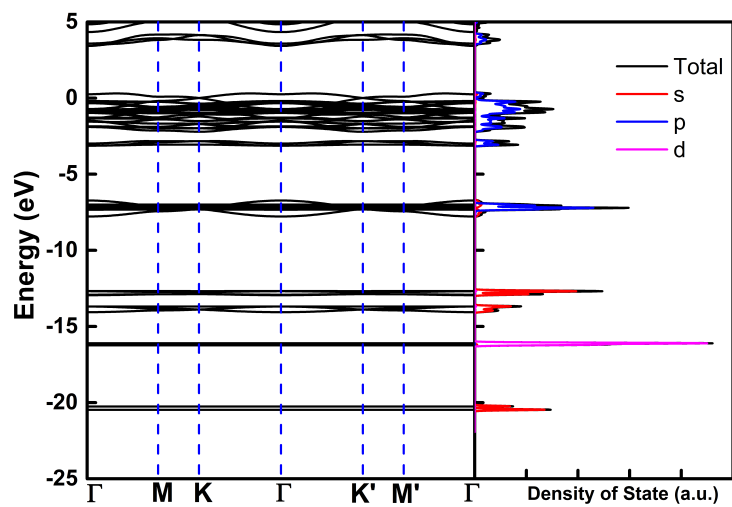
L. L. acknowledges the support from the National Science Fund for Distinguished Young Scholars of China (No. 61525404).

-
- * liulei@ciomp.ac.cn
 † shendz@ciomp.ac.cn
- ¹ P. R. Wallace, *Phys. Rev.* **71**, 622 (1947).
 - ² K. S. Novoselov, A. K. Geim, S. V. Morozov, D. Jiang, M. I. Katsnelson, I. V. Grigorieva, S. V. Dubonos, and A. A. Firsov, *Nature* **438**, 197 (2005).
 - ³ Y. B. Zhang, Y. W. Tan, H. L. Stormer, and P. Kim, *Nature* **438**, 201 (2005).
 - ⁴ B. A. Bernevig, T. L. Hughes, and S.-C. Zhang, *Science* **314**, 1757 (2006).
 - ⁵ D. Hsieh, D. Qian, L. Wray, Y. Xia, Y. S. Hor, R. J. Cava, and M. Z. Hasan, *Nature* **452**, 970 (2008).
 - ⁶ Y. L. Chen, J. G. Analytis, J. H. Chu, Z. K. Liu, S. K. Mo, X. L. Qi, H. J. Zhang, D. H. Lu, X. Dai, Z. Fang, S. C. Zhang, I. R. Fisher, Z. Hussain, and Z. X. Shen, *Science* **325**, 178 (2009).
 - ⁷ K. S. Novoselov, A. K. Geim, S. V. Morozov, D. Jiang, Y. Zhang, S. V. Dubonos, I. V. Grigorieva, and A. A. Firsov, *Science* **306**, 666 (2004).
 - ⁸ A. K. Geim and K. S. Novoselov, *Nat. Mater.* **6**, 183 (2007).
 - ⁹ A. K. Geim, *Science* **324**, 1530 (2009).
 - ¹⁰ A. H. Castro Neto, F. Guinea, N. M. R. Peres, K. S. Novoselov, and A. K. Geim, *Rev. Mod. Phys.* **81**, 109 (2009).
 - ¹¹ G. Brumfiel, *Nature* **458**, 390 (2009).
 - ¹² R. F. Service, *Science* **325**, 267 (2009).
 - ¹³ *Nat. Nanotech.* **5**, 755 (2010).
 - ¹⁴ P. Kim, *Nat. Mater.* **9**, 792 (2010).
 - ¹⁵ K. S. Novoselov, V. I. Fal'ko, L. Colombo, P. R. Gellert, M. G. Schwab, and K. Kim, *Nature* **490**, 192 (2012).
 - ¹⁶ R. F. Service, *Science* **348**, 490 (2015).
 - ¹⁷ E. Gibney, *Nature* **555**, 151 (2018).
 - ¹⁸ Y. Cao, V. Fatemi, S. Fang, K. Watanabe, T. Taniguchi, E. Kaxiras, and P. Jarillo-Herrero, *Nature* **556**, 43 (2018).
 - ¹⁹ D. Malko, C. Neiss, F. Vines, and A. Goerling, *Phys. Rev. Lett.* **108** (2012), 10.1103/PhysRevLett.108.086804.
 - ²⁰ S. Cahangirov, M. Topsakal, E. Akturk, H. Sahin, and S. Ciraci, *Phys. Rev. Lett.* **102**, 236804 (2009).
 - ²¹ F. Ma, Y. Jiao, G. Gao, Y. Gu, A. Bilic, Z. Chen, and A. Du, *Nano Lett.* **16**, 3022 (2016).
 - ²² J. Wang, S. Deng, Z. Liu, and Z. Liu, *Nat. Sci. Rev.* **2**, 22 (2015).
 - ²³ J. P. Perdew, K. Burke, and M. Ernzerhof, *Phys. Rev. Lett.* **77**, 3865 (1996).
 - ²⁴ P. E. Blochl, *Phys. Rev. B* **50**, 17953 (1994).
 - ²⁵ G. Kresse and J. Furthmuller, *Comput. Mater. Sci.* **6**, 15 (1996).
 - ²⁶ G. Kresse and J. Furthmuller, *Phys. Rev. B* **54**, 11169 (1996).
 - ²⁷ G. Kresse and D. Joubert, *Phys. Rev. B* **59**, 1758 (1999).
 - ²⁸ C. K. Moller, *Nature* **182**, 1436 (1958).
 - ²⁹ S. V. Morozov, K. S. Novoselov, M. I. Katsnelson, F. Schedin, D. C. Elias, J. A. Jaszczak, and A. K. Geim, *Phys. Rev. Lett.* **100**, 016602 (2008).
 - ³⁰ G. R. Yettapu, D. Talukdar, S. Sarkar, A. Swarnkar, A. Nag, P. Ghosh, and P. Mandal, *Nano Lett* **16**, 4838 (2016).
 - ³¹ F. Lazarini, *Acta Crystallographica Section B: Structural Crystallography and Crystal Chemistry* **33**, 2961 (1977).
 - ³² K. K. Bass, L. Estergreen, C. N. Savory, J. Buckeridge, D. O. Scanlon, P. I. Djurovich, S. E. Bradforth, M. E. Thompson, and B. C. Melot, *Inorg. Chem.* **56**, 42 (2017).
 - ³³ A. Singh, K. M. Boopathi, A. Mohapatra, Y. F. Chen, G. Li, and C. W. Chu, *ACS Appl. Mater. Interfaces* **10**, 2566 (2018).

Supplemental Information:
A simple rule for finding Dirac Cones in Bilayered Perovskites



SIFIG 1. The totally calculated electronic band structure of bulk CsPbBr₃, together with its orbit-decomposed DOS.



SIFIG 2. The totally calculated electronic band structure of a hexagonal CsPbBr₃ bilayer, together with its total and site-decomposed DOS.